Int. J. Bio-Inorg. Hybr. Nanomater., 9(4): 241-251, Winter 2021

Investigation on Photocatalytic Activity of Perovskite $ZnTiO_3$ and $CdTiO_3$ Nanocrystals for Degradation of Crystal Violet and Congo Red Pollutants under Sunlight

T. Tavakoli-Azar[1], A.R. Mahjoub[2], M. Seyed Sadjadi[3], N. Farhadyar[4], M. Hossaini Sadr[5]

[1,3] *Department of Chemistry, Science and Research Branch, Islamic Azad University, Tehran, Iran*
[2] *Department of Chemistry, Faculty of Basic Sciences, Tarbiat Modares University, Tehran, 14115–175, Iran*
[4] *Department of Chemistry, Varamin-Pishva Branch, Islamic Azad University, 33817-74895 Varamin, Iran*
[5] *Department of Chemistry, Faculty of Science, Azarbaijan Shahid Madani University, Tabriz, Iran*

Received: 23 September 2020; Accepted: 25 November 2020

ABSTRACT: Perovskite nanocrystals of $ZnTiO_3$ and $CdTiO_3$ with the cubic and orthorhombic structures were synthesized using the hydrothermal method. The crystal structures confirmed by XRD, morphology and particle size, chemical composition, and surface chemical features of samples synthesized are evaluated through, Fe-SEM, TEM, EDX , FT-IR, and BET analyzes. The average crystallites size $ZnTiO_3$ and $CdTiO_3$ perovskite were determined 12.03 and 43.7 nm, respectively by Debye Scherer's relationship.The Optical and photocatalytic properties of ZnTiO3 and $CdTiO_3$ are investigated by DRS (Differential reflectance spectroscopy) and UV-Vis analysis, respectively. The E_{bg} value (band gap energy) of the perovskites was obtained using Tauc plots. The cubic $ZnTiO_3$ showed E_{bg}=3.11 eV against the $CdTiO_3$ with E_{bg}=3.39 eV. The photocatalytic activities of perovskite $ZnTiO_3$ and $CdTiO_3$ nanocrystals were evaluated for degradation Congo red (CR) and Crystal violet (CV) pollutants. The $ZnTiO_3$ degraded both the CR and CV dyes with high efficiency (91% and 72%) compared with $CdTiO_3$ perovskite (51% and 9.7%) under 60 min of the sunlight irradiation. This high performance is affected by factors such as narrowing of the E_{bg}, the larger surface area, smaller crystal size and the existence of the hierarchical porous in the structure of the $ZnTiO_3$ than $CdTiO_3$. The kinetics studies revealed the rate constant of photodegradation of CR anionic dye by both of the perovskite as-synthesized is greater than degradation of cationic CV. The decomposition of the crystal violet fits the pseudo-first-order kinetic, while the degradation of the CR follows both the pseudo-first-order and the pseudo-second-order kinetic according to R^2> 0.9.

Keywords: *Azo dyes, $CdTiO_3$, Perovskite nanocrystal, Photocatalytic, $ZnTiO_3$*

INTRODUCTION

Perovskite metal oxides are compounds with formula ABO_3, where A^{2+} and B^{4+} are cations with different ionic radii. [1, 2]. Perovskite compounds are crystallized in various crystal lattices such as cubic, hexagonal, orthorhombic. Among perovskite structures, the cubic structure is one of the ideal structures for crystal lattices. In this kind of structures, the A cation with a larger ionic radii in the center of the crystal is coor-

(*) Corresponding Author - e-mail: tayebeh.tavakoliazar@srbiau.ac.ir

dinated with O anions, and B atoms with a smaller size are coordinated with anions in the corners of the crystal lattice [3]. The stability of the ABO_3 structures is predicted through the relation of (1).

$$t = r_A + r_O / \sqrt{(2(r_B + r_O)} \quad (1)$$

r_A, r_B, and r_O are ionic radius of ABO_3 atoms. The perovskite with cubic structure is stable in t=1, while it is distorted into orthorhombic, hexagonally, and tetragonal structures in 1>t>1 [4]. ABO_3-based perovskite are utilized in various aspects such as gas sensors, displays, solar cells, luminescence materials, catalysts as well as piezoelectric devices. Due to their optical, chemical, and magnetic properties, they are used in photocatalytic and photovoltaic systems [5, 6]. The titanium-based perovskite, such as $ZnTiO_3$ and $CdTiO_3$ semiconductors crystallize with cubic and orthorhombic structures, have been widely studied due to their potential applications in various aspects such as pigments, luminescence materials, catalysts, microwave dielectrics, and as the antibacterial [7-11]. Both the perovskite structures of $ZnTiO_3$ and $CdTiO_3$ are prepared via many methods: solid-state reaction [12], sol-gel [13], hydrothermal [14] and Co-Precipitation Process [15], Pechini method [16], and Sonochemical [17]. Despite the many synthetic methods, the hydrothermal method is great interest to researchers for preparation of inorganic semiconducting. That is utilized for obtaining compounds with a high percentage of purity, low energy consumption, high homogeneity, controlling particle size, lower pollution [18].

The dyes of the Congo red (CR) and Crystals violet (CV) utilized in this research are in the category azo dyes. These are found abundance in effluence. The CV dye is used in medical-biological, and textile industry. Crystal violet is a cationic dye susceptible to oxidation-reduction processes which leads to production toxic metabolites in water [19]. Congo red is utilized in the plastic, paper, and textile industries. It is an anionic dye that establishes strong interactions with cellulose. Nevertheless, its reactions create carcinogenic products that lead to severe harm to humans and the lives of organisms [20, 21]. Therefore, the degradation of such pollutants is one of the most important goals of scientists.

The purpose of this study is to prepared simple perovskite photocatalysts that could be active under sunlight irradiation. Efforts have been made to use accessible and renewable energy sources as well as simpler synthetic and lower-cost photocatalysts for the degradation of environmental pollutants. Therefore, $ZnTiO_3$ and $CdTiO_3$ perovskite with less construction energy and greater stability can be suitable semiconductors for the destruction of environmental pollutants under natural sunlight. In the present study, we have tried to investigate and compare the photocatalytic performance of $ZnTiO_3$ and $CdTiO_3$ perovskite for degradation of anionic and cationic dyes of Congo red and Crystal violet, which are very destructive to the environment.

EXPERIMENTAL

Materials

$ZnTiO_3$ and $CdTiO_3$ nanocrystals were prepared from the following inexpensive and accessible chemical: $ZnCl_2$ (Merck, ≥98%), $CdCl_2.H_2O$ (Sigma Aldrich ≥99%), and TiO_2 (Merck, ≥99%). That are the precursors of zinc, cadmium, and titanium metals, respectively. Congo red (CR) and also Crystal violet (CV), from Merck Company, employed as pollutions. The only solvent utilized in this research is distilled water.

Synthesis of the $ZnTiO_3$ and $CdTiO_3$ Nanocrystals

The $ZnTiO_3$ and $CdTiO_3$ nanocrystals were prepared through the hydrothermal method. 1.360 g of $ZnCl_2$ and 2.012 g of $CdCl_2.H_2O$ with 0.79 g of TiO_2 were utilized in 45 mL of distilled water separately. The final mixture was stirred during15 minutes to make the solution homogeneity. In the next phase, 3.35 g of Na OH was added to desired solutions and stirred for another 35 minutes. The beakers' contents were transferred into a Teflon-Line stainless autoclave with 100 cc capacity separately. The autoclaves put in the oven at 180 °C@24 h. After cooling the autoclave, the obtained precipitations were filtered by vacuum pump and washed with distilled water until the pH of the washing solution equals 7. The samples were dried at 90 °C@10 h. The obtained productions are calcined at 750 °C ($ZnTiO_3$) and 1050 °C ($CdTiO_3$) for 3 h.

Photocatalytic activity test

CV and CR were employed as wastewater pollutants for the evaluation of $ZnTiO_3$ and $CdTiO_3$ photocatalytic performance. The photocatalytic activities were investigated by using 0.03 g of $ZnTiO_3$ and $CdTiO_3$ photocatalysts in 30 ml of dye solutions with a concentration of 10 ppm under sunlight irradiation for 180 minutes. $ZnTiO_3$ and $CdTiO_3$ powders were added to Crystal violet and Congo red solutions. The resulting mixture is stirred for 35 min in the dark place to attain adsorption-desorption equilibrium between dye molecules and the surface of $ZnTiO_3$ and $CdTiO_3$ photocatalysts. In the next step, the samples are exposed to sunlight. After every 30 minutes of radiation, absorption changes are recorded by UV-Vis spectrometer at λ_{max} = 590 nm and λ_{max} = 499 nm for Crystal violet and Congo red, respectively. The percentages of dyes degradation by $ZnTiO_3$ and $CdTiO_3$ was achieved by relation (2):

$$D(\%) = \left(\frac{A_o - A_t}{A_o}\right) \times 100 \qquad (2)$$

Where, A_0 and A_t are the value of absorbance of dyes, before any reaction and after a time of sunlight irradiation, respectively. The rate constant (K) of CV and CR degradation was calculated by the pseudo-first-order, and also pseudo-second-order kinetics.

Characterization

The patterns of XRD were saved by the STOE STADI-P device with Cu Kα radiation (λ= 1.54060 Å). Fe-SEM and TEM were employed to determine the morphology and size of nano particles. EDX spectroscopy utilized for identification of the chemical composition of samples. DRS analysis and calculation of band gap energy values of semiconductors by Tauc's plots were down by UVS-2500. Ft-IR analyzes were stored by a nexus 870 spectroscopy. The determination of specific surface area and other parameters of BET are performed by the Belsorp mini II instrument. The results of photocatalytic experiments were collected by Carry-vin 100 spectrophotometer.

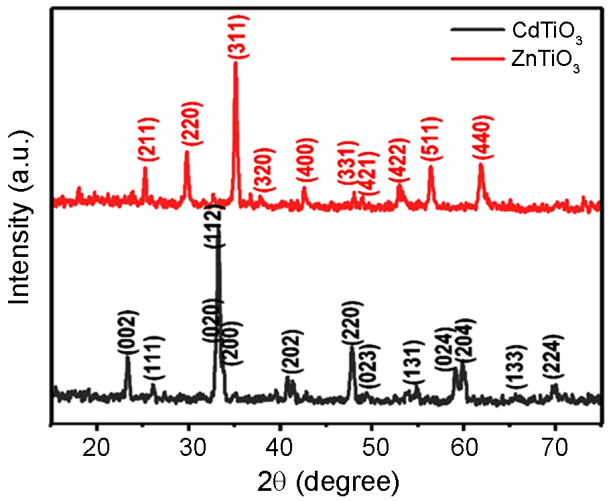

Fig. 1. XRD patterns of the $ZnTiO_3$ and $CdTiO_3$ perovskite.

RESULTS AND DISCUSION

Determination of nanocrystal structure

Fig. 1 showed the XRD patterns of $ZnTiO_3$ and $CdTiO_3$ perovskite prepared by the hydrothermal and annealed at high temperatures. The orthorhombic structure of the $CdTiO_3$ formed without any impurity in space group Pbnm that fitted with JCPDS card NO, 01-078-1014. The cubic structure of the $ZnTiO_3$ synthesized at 750 °C, which corresponds well with the JCPDS Card No. 00-039-0190. Generally, the synthesis of the pure $CdTiO_3$ and $ZnTiO_3$ perovskites without any secondary phases at such temperature is difficult. That is due to the evaporation of cadmium oxide and unstable cubic structures of $ZnTiO_3$ that are transformed to the hexagonal phase, and or may be decomposed to TiO_2 and Zn_2TiO_4 spinals.

Structural data achieved from XRD of the $ZnTiO_3$ and $CdTiO_3$ perovskite tabulated in Table1. The average crystallites size was determined by Debye Scherer's Eqn. (3):

Table 1. Structural data and crystalline parameters of the $ZnTiO_3$ and $CdTiO_3$

Sample	Crystallite size (nm)	Unit cell parameters (Å)			V(Å^3)
		a	b	c	
$ZnTiO_3$	12.033	8.469	8.469	8.469	607.43
$CdTiO_3$	43.766	5.322	5.388	7.610	218.216

$$D = (K\lambda) / (\beta \cos\theta) \quad (3)$$

Where, D presents Crystallites size, K is 0.9 (Scherer constant), λ = 0.15406 nm, β = FWHM in radians, and θ indicates peak position (radians). Crystalline parameters (a, b, and c) are achieved by the equations of the interplanar spacing (4) and (5), orthorhombic and cubic unit cells, respectively.

$$\frac{1}{d^2} = \frac{h^2}{a^2} + \frac{k^2}{b^2} + \frac{l^2}{c^2} \quad (4)$$

$$\frac{1}{d^2} = \frac{h^2 + k^2 + l^2}{a^2} \quad (5)$$

Where h, k, and l present the miller indicated. a, b, and c are lattice constants of unite cell. d is interplanar spacing.

FT-IR analysis

FT-IR spectra of the $ZnTiO_3$ and $CdTiO_3$ perovskite are exhibited in Fig. 2. Commonly, stretching vibrations of the Ti-O metal oxide in the TiO_6 octahedral group of the $ZnTiO_3$ and $CdTiO_3$ appear in 445-800 cm^{-1}. Cd-O vibrations are found in 425-440 cm^{-1} [22]. The two broad absorption peaks detected in the areas 1200-1600 cm^{-1} and 650 cm^{-1} are related to vibrations of the Cd-Ti-O and Ti-O bands, respectively [23,24]. In the $ZntiO_3$ compound, identified peaks at around 700-800 cm^{-1}, 650-650 cm^{-1}, and 407-469 cm^{-1} could be due to the vibrational modes of Zn-O-Ti, O-Ti-O, and Zn-O, respectively [25, 26].

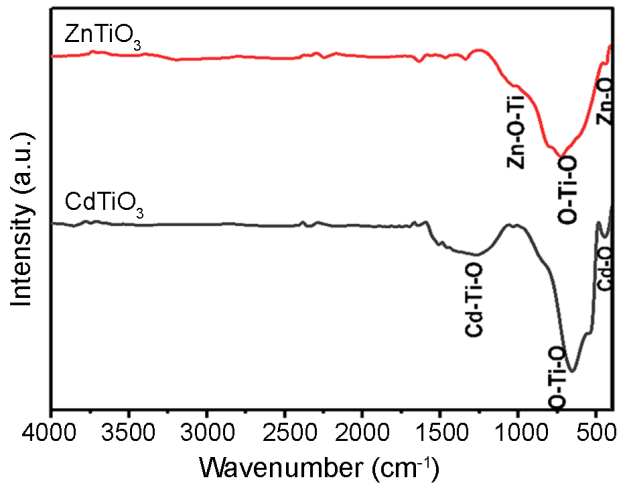

Fig. 2. Ft-IR spectra of the $ZnTiO_3$ and $CdTiO_3$ perovskites.

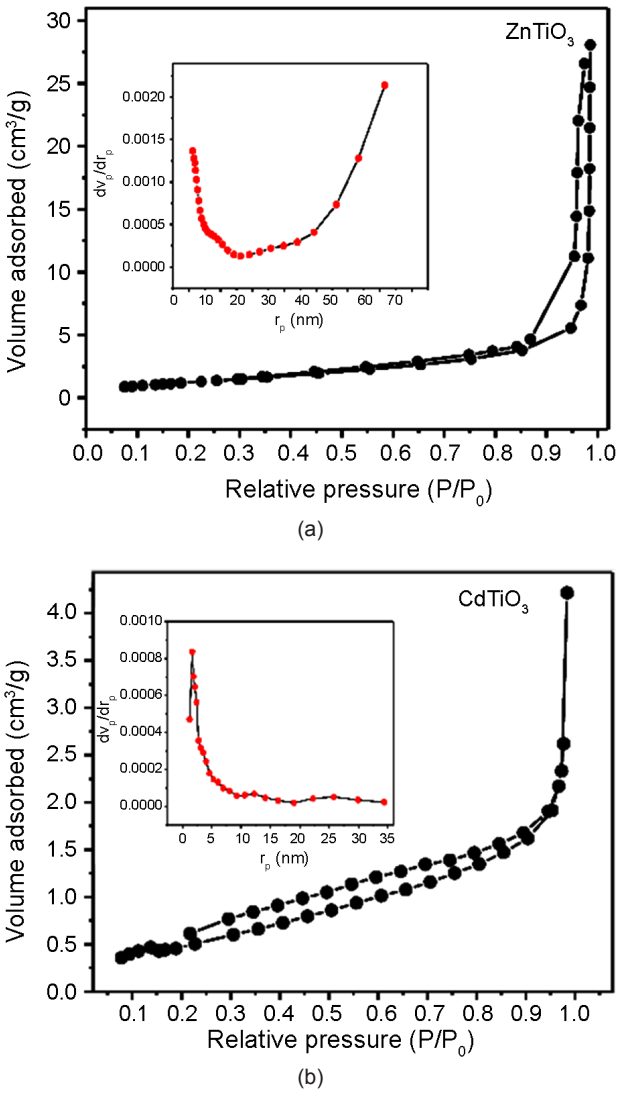

Fig. 3. N_2 adsorption-desorption isotherms of the $ZnTiO_3$ and $CdTiO_3$.

Porosity and Surface chemistry of the $ZnTiO_3$ and $CdTiO_3$ perovskites

In general, porosity and BET parameters (specific surface area, average pore diameters, and total pore volume) characterization are performed by Nitrogen adsorption/desorption isotherms. Fig. 3 shows adsorption/desorption isotherms of the $ZnTiO_3$ and $CdTiO_3$. Isotherms of both perovskites are of kind IV, according to the IUPAC classification. $ZnTiO_3$ indicates adsorption/desorption isotherm with hysteresis loop H_3 at relative pressures of 0.65 to 0.99. While $CdTiO_3$ shows isotherm with hysteresis loop H_4 in p/p_0 of 0.2 to 0.98.

The BET analysis results of the $ZnTiO_3$ and $CdTiO_3$ are listed in Table 2 indicate that $ZnTiO_3$ perovskite

Table 2. The BET analysis of synthesized perovskites.

Sample	$ZnTiO_3$	$CdTiO_3$
Average pore diameter (nm)	37.819	12.73
Total pore volume (cm3/g)	0.0434	0.00652
Surface area (m2/g)	4.595	2.048

has an average pore diameter and total pore volume are more considerable than $CdTiO_3$. Specific surface area of $ZnTiO_3$ more than twice of $CdTiO_3$, although this amount is not so significant. Commonly a perovskite compounds due to synthesis at high temperatures exhibit porosity and lower surface area.

The pore size distribution (PSD) curve of the $ZnTiO_3$, and $CdTiO_3$ were obtained by The Barrett-Joyner-Halenda method (BJH). The results presented in the inset of the Fig.4 indicate a uniform distribution of pore size, and also the existence of mesoporous (r_p= 4 nm) in the structure of $CdTiO_3$, while the pore size for $ZnTiO_3$ is distributed in r_p= 1.21-61 nm. The results confirm the existence of a combination of the pores of macro (>50 nm), and meso (2-50 nm). In other words, $ZnTiO_3$ compounds are hierarchical porous in structure. As a result, the increasing surface area and the existence of hierarchical porous features could be an important factors in enhancing photocatalytic performance [27, 28] because of additional photon absorption efficiency, and also effective insertion of molecules by the macro pores [29].

Morphology and particles size analysis

Fig. 4 and Fig. 5 show Fe-SEM and TEM images of the $ZnTiO_3$ and $CdTiO_3$ prepared at 750 °C and 1050 °C, respectively. In the images related to Fe-SEM of the $ZnTiO_3$ particles (Fig. 4a), is observed grains with a spherical morphology, particle size is almost less than 200 nm. $CdTiO_3$ (Fig. 4b) has plate-like morphology with thickness less than 300 nm.

TEM micrographs related to $ZnTiO_3$ particles in Fig. 5 display spherical-like morphology and with a size of less 200 nm, while the TEM image of $CdTiO_3$ (Fig. 5b) shows needle-like morphology with a size less 60 nm. The particles size indicated in TEM micrographs of $ZnTiO_3$ is much bigger than the average crystallite

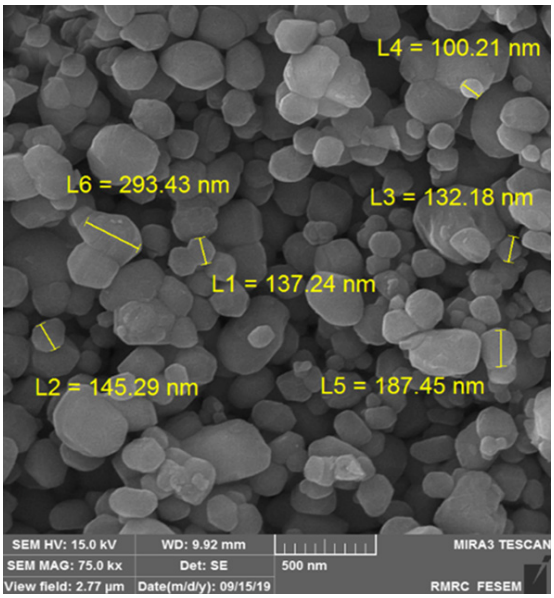

(a)

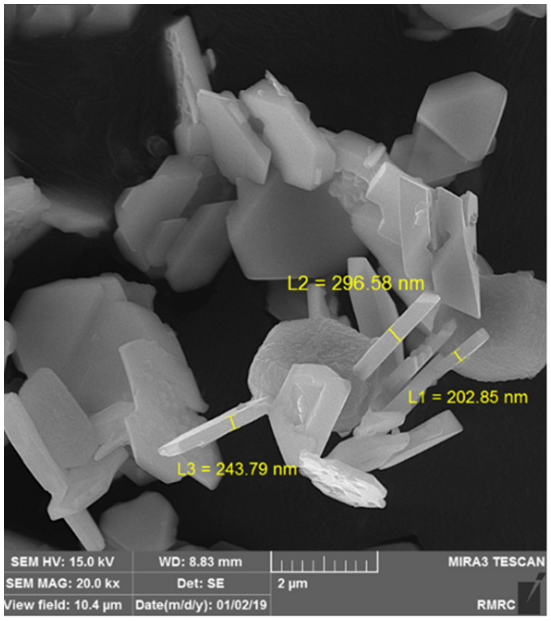

(b)

Fig. 4. FE-SEM image (a) $ZnTiO_3$, (b) $CdTiO_3$.

size achieved by XRD, because the particles observed by TEM are composed of smaller particles [30].

Optical properties

The DRS spectra of the $ZnTiO_3$ and $CdTiO_3$ are exhibited in Fig. 6. In the $ZnTiO_3$, the absorption peaks at 391 nm at 394 nm (shoulder) are seen. While in the $CdTiO_3$ spectrum, a maximum absorption peak was observed at 390 nm. The value of the band gap energy (E_{bg}) of the synthesized perovskite was achieved through the following equation (6):

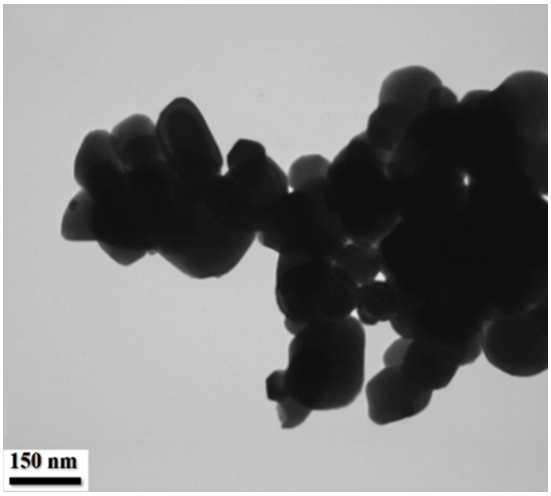

(a)

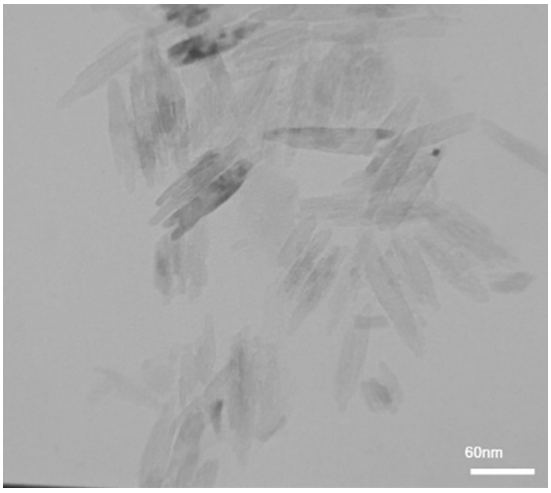

(b)

Fig. 5. TEM image (a) $ZnTiO_3$, (b) $CdTiO_3$.

$$(\alpha h\nu)^2 = K(h\nu - E_g) \quad (6)$$

Where hν presents photon energy, Eg represents band gap energy. α and K is the absorption coefficient and the effective masses of the valence band and conduction band, respectively [31].

The E_{bg} of the $ZnTiO_3$ and $CdTiO_3$ in the inset of Fig. 6 shows 3.11 eV and 3.39 eV, respectively. Since the activity of semiconductors with band gap energy of more than 3.2 eV is limited under visible light, it is expected that zinc titanate is more active compared with cadmium titanate under sunlight.

Investigation Photocatalytic activity of $ZnTiO_3$ and $CdTiO_3$

Photodegradation of both CR and CV dyes with 10 ppm concentration by the photocatalysts of $ZnTiO_3$

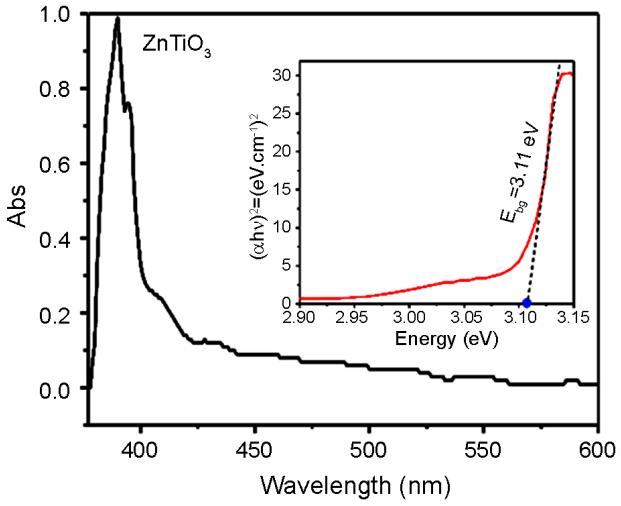

(a)

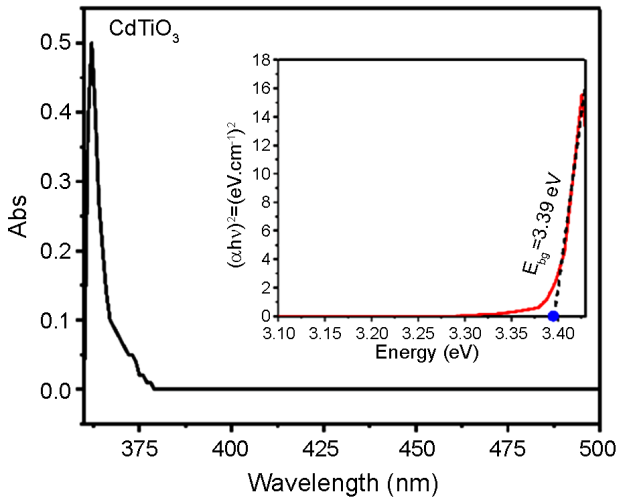

(b)

Fig. 6. DRS spectra of the $ZnTiO_3$ and $CdTiO_3$, and the value of band gap energy (inset).

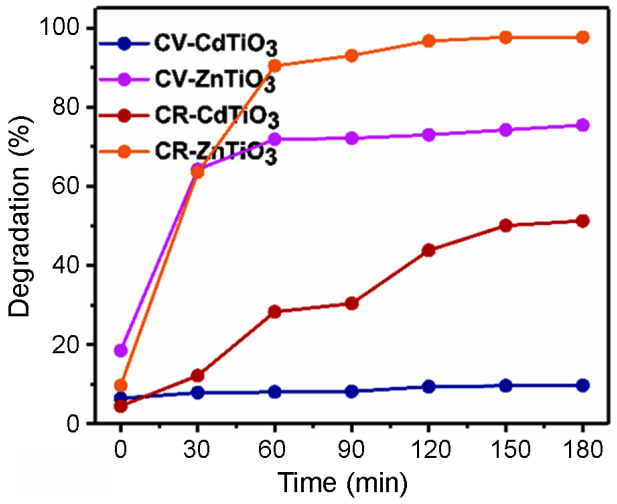

Fig. 7. Degradation of CR and CV dyes by $ZnTiO_3$ and $CdTiO_3$.

Table 3. Degradation CR and CV dyes by various photocatalysts.

Photocatalyst	Dye	Dye concentration	Photocatalyst concentration	Light source	Radiation Time	D%	Ref.
TiO_2	CR	4 ppm	0.1 g/250 ml	Solar	30 min	64.72	[32]
CdO	CR	5 ppm	0.01 g/25 ml	Visible	120 min	94	[33]
ZnO	CR	-	-	Visible	80 min	38	[34]
$PbTiO_3$	CR	-	-	Visible	150 min	92	[35]
$CdTiO_3$	CR	10 ppm	0.3 g/30 ml	Solar	60 min	51.27	This
$ZnTiO_3$	CR	10 ppm	0.3 g/30 ml	Solar	60 min	91	work
TiO_2	CV	5 ppm	1g/L	Visible	120 min	<10	[36]
CdO	CV	5 ppm	0.01 g/25 ml	Visible	60 min	15	[33]
ZnO	CV	5 ppm	0.1 g/40 ml	Visible	60 min	75.57	[37]
$CdTiO_3$	CV	10 ppm	0.3 g/30 ml	Solar	60 min	9.7	This
$ZnTiO_3$	CV	10 ppm	0.3 g/30 ml	Solar	60 min	72	work

and $CdTiO_3$ showed in Fig. 7. The results indicate that both CR and CV dyes degraded with high percentages by $ZnTiO_3$, 98% and 76%, respectively. While $CdTiO_3$ didn't show the better performance for degradation

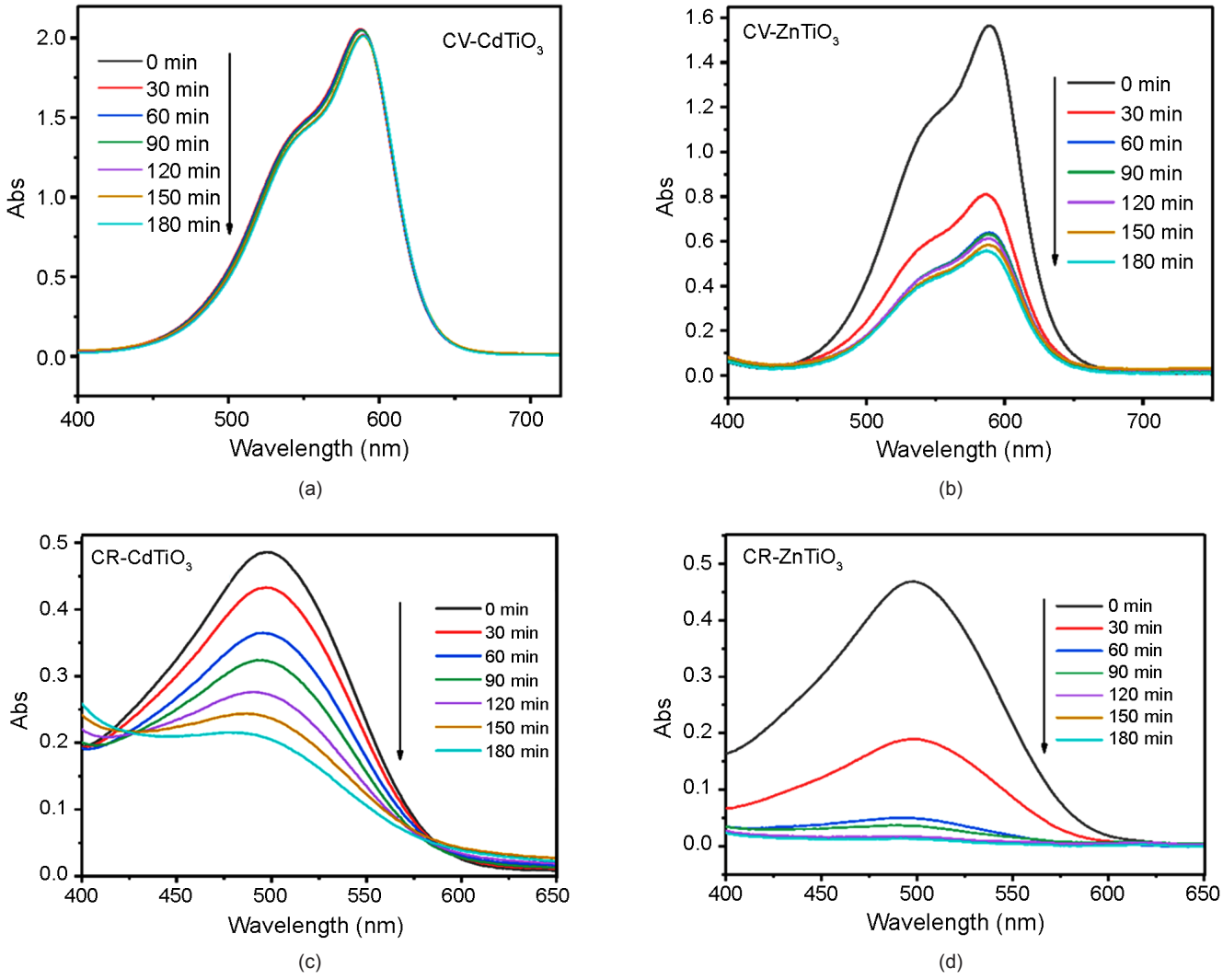

Fig. 8. Abs. Spectra of the CV and CR photodegradation versus time by $ZnTiO_3$ and $CdTiO_3$ under sunlight irradiation.

Table 4. Kinetics parameters of photodegradation of the CR and CV dyes.

Samples	Pseudo-first-order		Pseudo-second-order	
	R^2	$K\times10^{-4}$ (min^{-1})	R^2	$K\times10^{-4}$ (min^{-1})
CV-$CdTiO_3$	0.9053	30	0.7491	6E-.05
CV-$ZnTiO_3$	0.6220	51	0.7277	57
CR-$CdTiO_3$	0.9771	40	0.9081	101
CR-$ZnTiO_3$	0.8534	186	0.944	4891

this kind of pollutions, especially for CV dye (9.7%).

The degradation value of the CR and CV azo dyes by various synthesized photocatalysts is presented in Table 3. As found, $ZnTiO_3$ indicated excellent efficiency compared to other photocatalysts.

Kinetics investigations

Absorption spectra of the CR and CV photodegradation versus irradiation time present in Fig. 8. The results revealed, the strength of absorption peaks of the $ZnTiO_3$ decreased with more intensity compared with $CdTiO_3$ for both the CR and CV dyes at the $\lambda_{max\ (CR)}$= 499 nm and $\lambda_{max\ (CV)}$= 590 nm, respectively. The degradation efficiency of both the anionic and cationic dyes by $ZnTiO_3$ perovskite is higher than $CdTiO_3$. That could be due to the narrowing E_{bg}, increase of surface area, and existence of hierarchical porous in structure which is more effective in improving photocatalytic performance.

The kinetics investigations are depicted in Fig. 9. The constant rate of decomposition CR (k_{CR}) and CV (k_{CV}) in photocatalytic processes was computed through the pseudo-first-order (7) and pseudo-second-order models (8).

$$\ln\left(\frac{A_o}{A_t}\right) = kt \tag{7}$$

$$\frac{1}{A_t} = \frac{1}{A_o} + kt \tag{8}$$

Where k representing rate constant (min^{-1}) is achieved via slope $\ln(A_0/A_t)$ and $1/A_t$ plots versus time. A_0 presents initial absorption of dye, and A_t is intensity absorption in certain times of the reaction process, t indicate the reaction time [38].

The results of kinetics studies are listed in Table 4, present that the CV degradation by $CdTiO_3$ follows pseudo-first-order with R^2> 0.9. In contrast the degradation of CR fits both pseudo-first-order and pseudo-second-order kinetics by $CdTiO_3$ and $ZnTiO_3$.

The maximum amount of K was obtained for decomposition of the CR by $ZnTiO_3$ (K_{CR}= 4891.10^{-4} min^1), while the least amount was achieved for degradation of the CV by $CdTiO_3$. As a result, the efficiency of photodegradation of both the dye by the $ZnTiO_3$ photocatalyst is better than $CdTiO_3$ under sunlight.

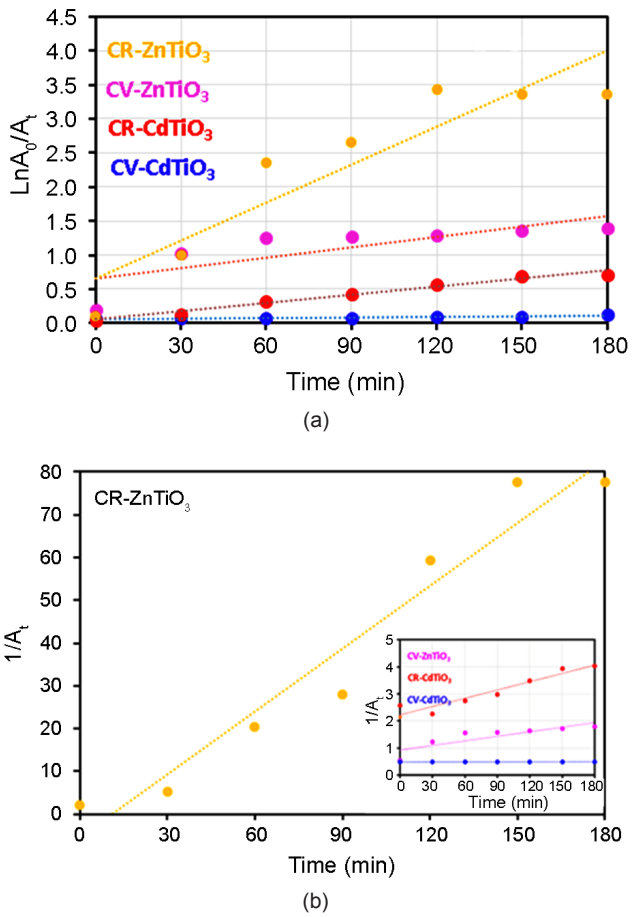

Fig. 9. Pseudo–first-order (a) and second-order kinetics charts (b) for photodegradation of the CR and CV dyes.

CONCLUSIONS

In this study, two nanocrystalline of $ZnTiO_3$ and $CdTiO_3$ perovskite with structures of cubic and orthorhombic were synthesized via the hydrothermal-annealing method. The average size $ZnTiO_3$ and $CdTiO_3$ nanocrystals were determined 12.06 and 43.7 nm, respectively. Optic and photocatalytic properties are both the perovskite investigated. The E_{bg} value of perovskite was achieved using Tauc plots. $ZnTiO_3$ showed E_{bg}= 3.11 eV which is lower than the $CdTiO_3$ with E_{bg}= 3.39 eV. The photocatalytic performance of $ZnTiO_3$ and $CdTiO_3$ was evaluated. The $ZnTiO_3$ degraded Congo red and Crystal violet dyes with high efficiency (91% and 72%) compared with $CdTiO_3$ (51% and 9.7%) under 60 min of sunlight irradiation. The excellent performance of $ZnTiO_3$ not only improved by the narrowing of the E_{bg} but also the other factors such as the larger surface area and hierarchical porous in the $ZnTiO_3$ structure were effective. Kinetics investigations show that; $ZnTiO_3$ followed pseudo-second-order kinetics for photodegradation Congo red. The degradation rate constant of Cong o red, by $ZnTiO_3$ (k_{CR} = 4891.10^{-4} min^{-1}) was more than $CdTiO_3$ (k_{CR}=101.10^{-4} min^{-1}).

REFERENCES

[1] B. Madhavan, A. Ashok, Review on nanoperovskites: materials, synthesis, and applications for proton and oxide ion conductivity, Ionics, 21 (2015) 601-610.

[2] S.F. Hoefler, G. Trimmel, T. Rath, Progress on lead-free metal halide perovskites for photovoltaic applications: a review, Monatshefte für Chemie-Chemical Monthly, 148 (2017) 795-826.

[3] P. Kanhere, Z. Chen, A review on visible light active perovskite-based photocatalysts, Molecules, 19 (2014) 19995-20022.

[4] C.J. Bartel, C. Sutton, B.R. Goldsmith, R. Ouyang, C.B. Musgrave, L.M. Ghiringhelli, M. Scheffler, New tolerance factor to predict the stability of perovskite oxides and halides, Science advances, 5 (2019) eaav0693.

[5] D. Kumar, R.S. Yadav, A.K. Singh, S.B. Rai, Synthesis Techniques and Applications of Perovskite Materials, Perovskite Materials, Devices and Integration, IntechOpen2020.

[6] N. Jaykhedkar, V. Shah, S. Premkumar, First-principles study of polarization and piezoelectric properties of $PbZrO_3$, AIP Conference Proceedings, AIP Publishing LLC, 2018, pp. 140058.

[7] Y. Yan, H. Gao, J. Tian, F. Tan, H. Zheng, W. Zhang, Ferromagnetic Enhancement in $ZnTiO_3$ films induced by Co doping, Ceramics International, 45 (2019) 11309-11315.

[8] S. Lei, H. Fan, X. Ren, J. Fang, L. Ma, Z. Liu, Novel sintering and band gap engineering of ZnTiO 3 ceramics with excellent microwave dielectric properties, Journal of Materials Chemistry C, 5 (2017) 4040-4047.

[9] S.F. Wang, F. Gu, M.K. Lü, W.G. Zou, S.W. Liu, D. Xu, D.R. Yuan, G.J. Zhou, Photoluminescence characteristics of $ZnTiO_3$: Bi3+ nanocrystals, Journal of Physics and Chemistry of Solids, 65 (2004) 1243-1245.

[10] J. Yu, D. Li, L. Zhu, X. Xu, Application of $ZnTiO_3$ in quantum-dot-sensitized solar cells and numerical simulations using first-principles theory, Journal of Alloys and Compounds, 681 (2016) 88-95.

[11] A. Stoyanova, H. Hitkova, A. Bachvarova-Nedelcheva, R. Iordanova, N. Ivanova, M. Sredkova, Synthesis, photocatalytic and antibacterial properties of nanosized $ZnTiO_3$ powders obtained by different sol-gel methods, Digest Journal of Nanomaterials and Biostructures, 7 (2012).

[12] B. Lokesh, S. Kaleemulla, N.M. Rao, Synthesis and characterization of zinc titanates by solid state reaction, Int. J. Chem. Tech. Res, 6 (2014) 1929-1932.

[13] M. Salavati-Niasari, F. Soofivand, A. Sobhani-Nasab, M. Shakouri-Arani, A.Y. Faal, S. Bagheri, Synthesis, characterization, and morphological control of $ZnTiO_3$ nanoparticles through sol-gel processes and its photocatalyst application, Advanced Powder Technology, 27 (2016) 2066-2075.

[14] Y. Xin, C.-l. ZHAO, Y.-l. ZHOU, Z.-j. WU, J.-m. YUAN, W.-s. LI, Synthesis and characterization of $ZnTiO_3$ with high photocatalytic activity, Transactions of Nonferrous Metals Society of

China, 25 (2015) 2272-2278.

[15] P. Sirajudheen, K. Sanoop, M. Rashid, Visible Light Induced ZnTiO 3 Photocatalyst Synthesized by Co-Precipitation Process, Recent Advances in Chemical Engineering, Springer2016, pp. 227-234.

[16] Y.-S. Chang, Y.-H. Chang, I.-G. Chen, G.-J. Chen, Y.-L. Chai, Synthesis and characterization of zinc titanate nano-crystal powders by sol–gel technique, Journal of Crystal growth, 243 (2002) 319-326.

[17] C. Wattanawikkam, W. Pecharapa, Sonochemical synthesis, characterization, and photocatalytic activity of perovskite $ZnTiO_3$ nanopowders, IEEE transactions on ultrasonics, ferroelectrics, and frequency control, 63 (2016) 1663-1667.

[18] W. Shi, S. Song, H. Zhang, Hydrothermal synthetic strategies of inorganic semiconducting nanostructures, Chemical Society Reviews, 42 (2013) 5714-5743.

[19] A.M. Campos, P.F. Riaño, D.L. Lugo, J.A. Barriga, C.A. Celis, S. Moreno, A. Pérez, Degradation of crystal violet by Catalytic Wet Peroxide Oxidation (CWPO) with mixed Mn/Cu oxides, Catalysts, 9 (2019) 530.

[20] M.R. Sankar, V. Sivasubramanian, Application of statistical design to optimize the electrocoagulation of synthetic Congo red dye solution and predicting the mechanism, International Journal of Environmental Science and Technology, 17 (2020) 1373-1386.

[21] A. Yadav, M. Bhagat, V.Y. Seema, Congo Red Dye Removal From Aqueous Solution Using Activated Orange Peel, (2017).

[22] T. Acharya, R. Choudhary, Development of ilmenite-type electronic material CdTi0 3 for devices, IEEE Transactions on Dielectrics and Electrical Insulation, 22 (2015) 3521-3528.

[23] Z. Wu, Y. Zhang, X. Wang, Z. Zou, Ag@ SrTiO 3 nanocomposite for super photocatalytic degradation of organic dye and catalytic reduction of 4-nitrophenol, New Journal of Chemistry, 41 (2017) 5678-5687.

[24] J.-M. Zhu, M. Hosseini, A. Fakhri, S.S. Rad, T. Hadadi, N. Nobakht, Highly efficient of molybdenum trioxide-cadmium titanate nanocomposites for ultraviolet light photocatalytic and antimicrobial application: Influence of reactive oxygen species, Journal of Photochemistry and Photobiology B: Biology, 191 (2019) 75-82.

[25] K. Sahbeni, I. Sta, M. Jlassi, M. Kandyla, M. Hajji, M. Kompitsas, W. Dimassi, Annealing temperature effect on the physical properties of titanium oxide thin films prepared by the sol-gel method, J Phys Chem Biophys, 7 (2017) 2161-0398.1000257.

[26] K. Pugazhendhi, S. D'Almeida, P.N. Kumar, J.S.S. Mary, T. Tenkyong, D. Sharmila, J. Madhavan, J.M. Shyla, Hybrid TiO2/ZnO and TiO2/Al plasmon impregnated ZnO nanocomposite photoanodes for DSSCs: synthesis and characterisation, Materials Research Express, 5 (2018) 045053.

[27] H.T. Kim, M.T. Lanagan, Structure and microwave dielectric properties of (Zn1− xCox) TiO_3 ceramics, Journal of the American Ceramic Society, 86 (2003) 1874-1878.

[28] K.H. Reddy, S. Martha, K. Parida, Erratic charge transfer dynamics of Au/ZnTiO 3 nanocomposites under UV and visible light irradiation and their related photocatalytic activities, Nanoscale, 10 (2018) 18540-18554.

[29] H. Wang, H. Liu, S. Wang, L. Li, X. Liu, Influence of tunable pore size on photocatalytic and photoelectrochemical performances of hierarchical porous TiO2/C nanocomposites synthesized via dual-Templating, Applied Catalysis B: Environmental, 224 (2018) 341-349.

[30] M. Jose, M. Elakiya, S.M.B. Dhas, Structural and optical properties of nanosized ZnO/ZnTiO 3 composite materials synthesized by a facile hydrothermal technique, Journal of Materials Science: Materials in Electronics, 28 (2017) 13649-13658.

[31] K.H. Abass, $Fe2O_3$ thin films prepared by spray pyrolysis technique and study the annealing on its optical properties, International Letters of Chemistry, Physics and Astronomy, 6 (2015) 24-31.

[32] N. Harun, M. Rahman, W. Kamarudin, Z. Irwan, A. Muhammud, N. Akhir, M. Yaafar, Photocatalytic degradation of Congo red dye based on titanium dioxide using solar and UV lamp, Journal

of Fundamental and Applied Sciences, 10 (2018) 832-846.

[33] A. Tadjarodi, M. Imani, H. Kerdari, K. Bijanzad, D. Khaledi, M. Rad, Preparation of CdO rhombus-like nanostructure and its photocatalytic degradation of azo dyes from aqueous solution, Nanomaterials and Nanotechnology, 4 (2014) 16.

[34] C. Ankush, V. Ritesh, K. Swati, A. Sharma, S. Pooja, L. Xiangkai, B.K. Mujasam, I. Ahamad, K. Saurabh, R. Kumar, Photocatalytic dye degradation and antimicrobial activities of Pure and Ag-doped ZnO using Cannabis sativa leaf extract, Scientific Reports (Nature Publisher Group), 10 (2020).

[35] U.O. Bhagwat, J.J. Wu, A.M. Asiri, S. Anandan, Photocatalytic Degradation of Congo Red Using $PbTiO_3$ Nanorods Synthesized via a Sonochemical Approach, ChemistrySelect, 3 (2018) 11851-11858.

[36] S. Janitabar-Darzi, A. Mahjoub, Visible-light-active nitrogen doped TiO_2 nanoparticles prepared by sol-gel acid catalyzed reaction, Iranian Journal of Materials Science and Engineering, 9 (2012) 17-23.

[37] M.A. Habib, M. Muslim, M.T. Shahadat, M.N. Islam, I.M.I. Ismail, T.S.A. Islam, A.J. Mahmood, Photocatalytic decolorization of crystal violet in aqueous nano-ZnO suspension under visible light irradiation, Journal of Nanostructure in Chemistry, 3 (2013) 70.

[38] N. Khorshidi, S.A. Khorrami, M.E. Olya, F. Mottiee, Photodegradation of basic dyes using nanocomposite (Ag-zinc oxide-copper oxide) and kinetic studies, Oriental Journal of Chemistry, 32 (2016) 1205.

AUTHOR (S) BIOSKETCHES

Tayebeh Tavakoli-Aza, PhD., Department of Chemistry, Science and Research Branch, Islamic Azad University, Tehran, Iran, *Email: tayebeh.tavakoliazar@srbiau.ac.ir, tayebeh_tavakoliazar@yahoo.com*

Ali Reza Mahjoub, Professor, Department of Chemistry, Faculty of Basic Sciences, Tarbiat Modares University, Tehran, 14115–175, Iran, *Email: mahjouba@modares.ac.ir*

Mirabdullah Seyed Sadjadi, Professor, Department of Chemistry, Science and Research Branch, Islamic Azad University, Tehran, Iran, *Email: Msadjadi@srbiau.ac.ir*

Nazanin Farhadyar, Associate Professor, Department of Chemistry, Varamin-Pishva Branch, Islamic Azad University, 33817-74895 Varamin, Iran, *Email: quantomlife@gmail.com*

Moayad Hossaini Sadr, PhD., Department of Chemistry, Faculty of Science, Azarbaijan Shahid Madani University, Tabriz, Iran, *Email: hosainis@yahoo.com*